

Article

Characteristics of the Dye-Sensitized Solar Cells Using TiO₂ Nanotubes Treated with TiCl₄

Jun Hyuk Yang, Chung Wung Bark, Kyung Hwan Kim and Hyung Wook Choi *

Department of Electrical Engineering, Gachon University, Seongnam-Si, Gyeonggi-Do 461-701, Korea; E-Mails: hyuk1349@gmail.com (J.H.Y.); bark@gachon.ac.kr (C.W.B.); khkim@gachon.ac.kr (K.H.K.)

* Author to whom correspondence should be addressed; E-Mail: chw@gachon.ac.kr; Tel.: +82-31-750-5562; Fax: +82-31-750-8833.

Received: 27 January 2014; in revised form: 24 April 2014 / Accepted: 29 April 2014 /

Published: 5 May 2014

Abstract: The replacement of oxide semiconducting TiO₂ nano particles with one dimensional TiO₂ nanotubes (TNTs) has been used for improving the electron transport in the dye-sensitized solar cells (DSSCs). Although use of one dimensional structure provides the enhanced photoelectrical performance, it tends to reduce the adsorption of dye on the TiO₂ surface due to decrease of surface area. To overcome this problem, we investigate the effects of TiCl₄ treatment on DSSCs which were constructed with composite films made of TiO₂ nanoparticles and TNTs. To find optimum condition of TNTs concentration in TiO₂ composites film, series of DSSCs with different TNTs concentration were made. In this optimum condition (DSSCs with 10 wt% of TNT), the effects of post treatment are compared for different TiCl₄ concentrations. The results show that the DSSCs using a TiCl₄ (90 mM) post treatment shows a maximum conversion efficiency of 7.83% due to effective electron transport and enhanced adsorption of dye on TiO₂ surface.

Keywords: TiO₂ nanoparticle; anodic oxidation; TiO₂ nanotube; TiCl₄; dye-sensitized solar cells

1. Introduction

Since their invention in 1991, dye-sensitized solar cells (DSSCs) have been extensively studied as an alternative to silicon-based solar cells, owing to their simple structure, transparency, flexibility, low

production cost, and wide range of application. Despite these advantages, the low efficiency of DSSCs compared to that of silicon-based cells has limited their commercial implementation [1–4]. Consequently, there is a critical need to improve the efficiency of state-of-the-art DSSCs in order to realize next generation solar cells.

DSSCs are composed of four parts as follows: (1) the electrode film layer (TiO_2), covered by a monolayer of dye molecules, that absorbs solar energy; (2) the conductive transparent conductive oxide layer that facilitates charge transfer from the electrode layer; (3) the counter electrode layer made of Pt or C; (4) the redox electrolyte layer for reducing the level of energy supplied from the dye molecules [5,6]. Thus, research efforts to improve the efficiency of DSSCs have primarily been focused on improvements of the each DSSC component [7]. However, due to synergetic effects of its subcomponents, the enhancement of only one component might not be sufficient to improve efficiency of entire cell.

The interconnected TiO_2 nanoparticle is widely used as the mesoporous electrode film layer, because it is beneficial for adsorption large amount of dye molecules due to its large surface areas. However, the overall performance of DSSCs can be limited by the electron transport in the nanocrystal boundaries of TiO_2 nanoparticles and the electron recombination with the electrolyte during the electron migration process. To avoid this problem, many researchers have reported that one dimensional nanostructures can be used in DSSCs as replacements of nanoparticles to facilitate electron transfer [8–14]. In addition to their unique electron properties, one-dimensional TiO_2 nanostructures also function as light scattering materials. Nevertheless, dye adsorption in the one dimensional structure should be sacrificed due to the reduction of surface area.

In this work, we have considered combined strategies to improve the efficiency of DSSCs. We used oxide semiconductors in the form of TiO_2 nanotube (TNTs) to improve the electron transport through the film. Though a higher photoelectrical performance was obtained, we believe that further improvements in the photoelectrical performance of DSSCs could be achieved. To overcome reduced dye adsorption in one dimensional structure, we investigated the effects of TiCl_4 post treatment on DSSCs, combined with variations in the concentration of TNTs in TiO_2 nanoparticle/TNT composites. Consequently, this approach can be used for effectively increasing the dye adsorption of TiO_2 films.

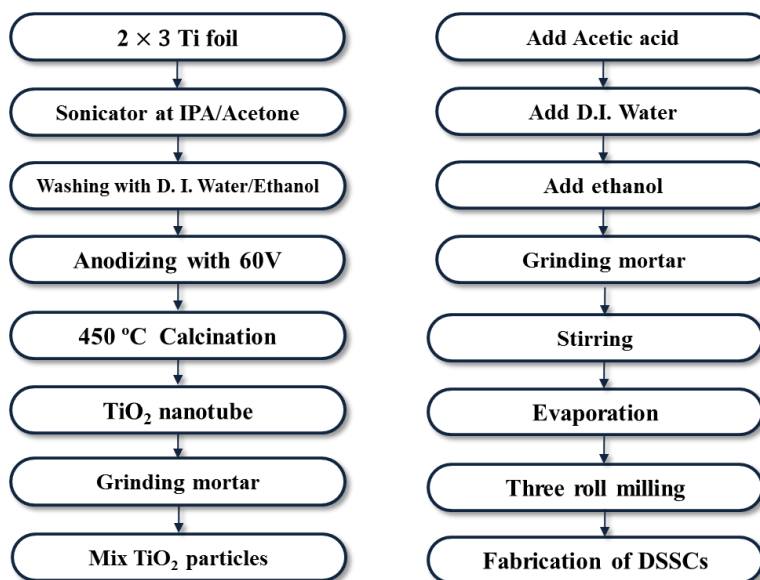
2. Experimental Section

TNTs were prepared by an optimized three step anodization process. Ti foil (0.25 mm thickness, 99.7% purity, Sigma-Aldrich, St. Louis, MO, USA) with an area of $2\text{ cm} \times 3\text{ cm}$ was degreased by ultrasonic agitation in acetone, isopropanol, and deionized water for 15 min each and then dried with N_2 gas. The ethylene glycol electrolyte contained 0.25 wt% NH_4F (98%, Sigma-Aldrich, St. Louis, MO, USA) and 2 vol% deionized water. The anodization was performed in a two electrode system where the Ti foil served as the working electrode and a Pt plate as the counter electrode. Anodization was conducted at room temperature at a constant voltage of 60 V, as shown in Figure 1. In order to obtain powders, the fabricated TNTs had to be detached from the Ti sheet in a H_2O_2 solution. The anodic oxidation was repeated many times to obtain the required amount of TNT powder. To achieve TNT powder of the desired crystallinity, the powder was calcined in air at $450\text{ }^\circ\text{C}$ for 3 h then the samples were milled with a mortar and pestle. Following this, the TiO_2 nanoparticles (Anatase 99.9%,

Sigma-Aldrich, St. Louis, MO, USA), and the TNT powder were mixed in various ratios (5–20 wt%) and ground in a mortar.

In addition, TiO₂ paste was prepared by combining TiO₂ nanoparticles with TNT powder. The prepared TiO₂ paste was coated onto FTO-glass (Fluorine-doped tin oxide coating glass) by a doctor blade. The TiO₂ coated substrate was calcined at 250 °C for 15 min and then at 450 °C for 15 min to promote crystal growth and remove organic constituents.

Figure 1. Flow chart of manufacturing dye-sensitized solar cells (DSSCs).



TiO₂ films were dipped for 30 min in a 30–120 mM TiCl₄ aqueous solution at 70 °C which was prepared by adding titanium tetrachloride (Sigma-Aldrich, St. Louis, MO, USA) to precooled distilled water in an ice bath. Following the post treatment, the TiO₂ film was annealed at 450 °C for 15 min.

A Pt catalyst electrode was prepared by mixing H₂PtCl₆ (5 mM, Sigma-Aldrich, St. Louis, MO, USA) in isopropyl alcohol with an ultrasonic treatment. A counter electrode, which facilitates the redox reaction of the electrolyte, was fabricated by spin coating the H₂PtCl₆ solution at 1000 rpm for 30 s, and annealed at 450 °C for 30 min.

The dye solution to be adsorbed on the electrode films was prepared by mixing 0.5 mM Ru-dye (N719, Solaronix, Rue de l'Ouriette, Aubonne, Switzerland) with ethanol. To facilitate the adsorption of the dye molecules, the prepared TiO₂ electrode films were placed in the dye solution in darkness for 24 h.

Finally, the DSSC was fabricated by sandwiching the prepared electrode film and counter electrode at 120 °C for 10 min using a hot melt sealant (60 °C). The electrolyte (I⁻/I₃⁻) was injected between the two electrodes with the inlet then sealed by a cover glass.

The phase of the TNTs obtained by anodization was examined by X-ray diffraction (XRD), using a Rigaku D/max-2200 diffractometer (Rigaku, Tokyo, Japan) with a CuK α radiation source. The morphology of the prepared TiO₂ films was investigated by field-emission scanning electron microscopy (FE-SEM, Hitachi S-4700, Tokyo, Japan) and the optical transmittance of the prepared TiO₂ electrode films was measured using a UV-Vis spectrometer (Perkin Elmer Lambda 750, Waltham, MA, USA). The conversion efficiency and electrochemical impedance spectroscopy (EIS,

Mcscience K3400, Suwon-si, Gyeonggi-do, Korea) of the fabricated DSSCs were measured using an $I-V$ solar simulator (McScience K3000, Suwon-si, Gyeonggi-do, Korea). The active area of the resulting cell exposed to light was approximately 0.25 cm^2 ($0.5 \text{ cm} \times 0.5 \text{ cm}$).

3. Results and Discussion

Figure 2 shows the XRD pattern of the Ti foil (JCPDS No. 44-1294) and of the TNT array by calcination at $450 \text{ }^\circ\text{C}$. After anodization, the TNT array peeled off from the Ti substrate and was analyzed and tested by XRD. The diffraction peaks of TNT array are in good agreement with the standard JCPDS cards of anatase TiO_2 (No. 21-1272). The XRD pattern of the TNT array shows (101), (004), (200), (105), (211), (204), (116), (220) and (215) anatase peaks.

Figure 2. XRD patterns of (a) Ti foil and (b) a TiO_2 nanotube array.

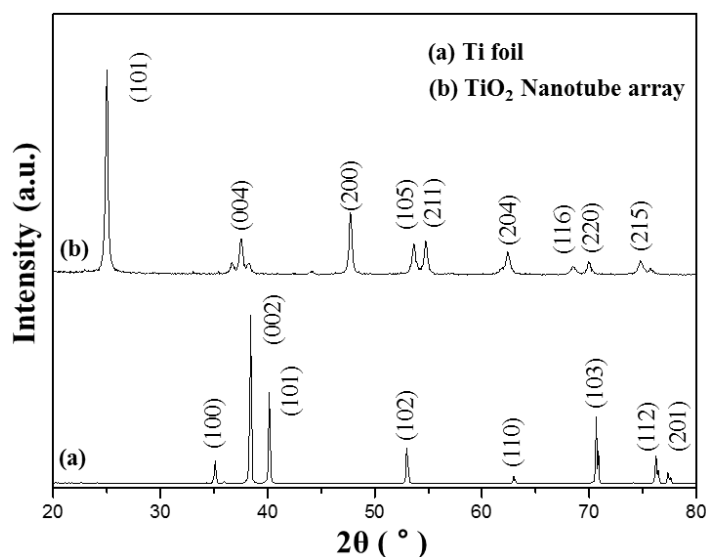


Figure 3a shows the SEM images of TiO_2 nanoparticles. The TiO_2 particle size is about 20–30 nm. Figure 3b indicates that the TNT diameter is about 120 nm, and the TNT surface is uniform. Additionally, for anodic oxidation at present conditions, the TNTs can come to a length of 40–45 μm as shown in Figure 3c. It is obvious that the TiO_2 nanoparticles, TNTs, and the substrate are well linked, which is helpful for the quick electron transportation in the film. Figure 3d shows the length of TNTs in a TiO_2 nanoparticle/TNT mixture to be approximately 1 μm .

Figure 4 shows the electrochemical impedance spectroscopy (EIS) analysis of TiO_2 nanoparticles/TNTs obtained at various weight ratios, which provides information about the electron transport and recombination in DSSCs. Two typical semicircles are observed in Nyquist plots, the small semicircular in the high frequency ranges and the large semicircular in the low frequency ranges correspond to the resistances of Pt/electrolyte interface and electrolyte/dye/ TiO_2 interface. The small semicircle is fit to a charge-transfer resistance (R_{CT1}) and constant phase, while the large semicircle is fit to a transfer resistance (R_{CT2}) and constant phase. As R_{CT1} is not affected by the use of TiO_2 nanoparticles/TNTs, we focused on the variations in R_{CT2} . The first semicircle is a minimum for the TNTs (10 wt%), which is related to charge-transfer resistance of the FTO/ TiO_2 and TiO_2 /electrolyte interfaces (R_{CT2}). The observed decrease in R_{CT2} of TNTs (10 wt%) indicates a reduction in electron recombination and

enhancement in the efficiency of electron transport. However, in the case of the TNTs (15 wt%), R_{CT2} increased with increasing of TNTs (15 wt%), due to the increase of trap sites which obstructs the movement of electrons from the TiO_2 film to the photoelectrode [15–18].

Figure 3. Field-emission scanning electron microscopy (FE-SEM) images of (a) TiO_2 nanoparticles; (b) the surface of a TiO_2 nanotube array; (c) a section of a TiO_2 nanotube array; (d) and a TiO_2 nanoparticle/ TiO_2 nanotube (TNT) composite film.

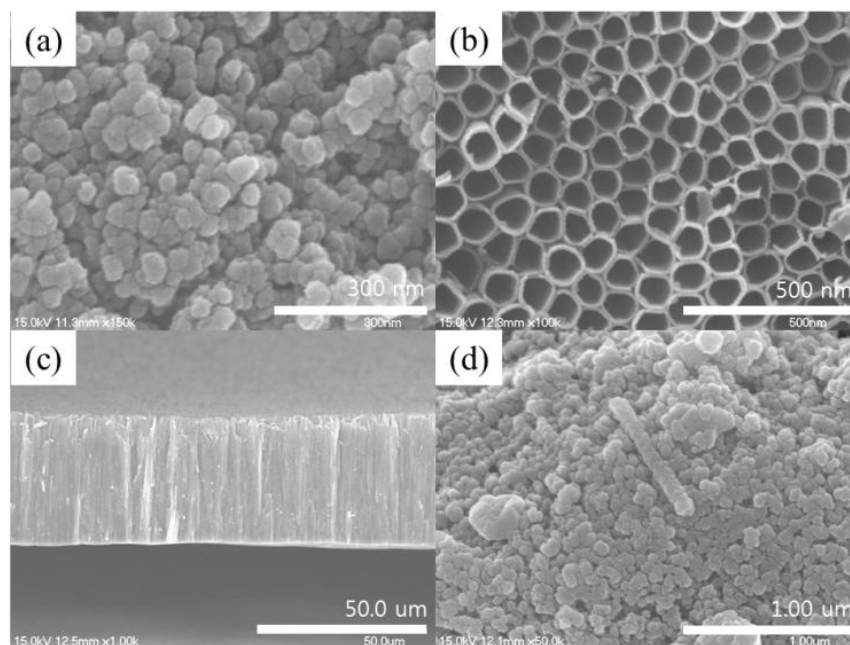


Figure 5 shows the current-voltage photovoltaic performance of DSSCs composed of bare TiO_2 nanoparticles and TNTs (5–20 wt%) under AM 1.5 illumination (100 mW/cm^2). Table 1 summarizes the efficiency, fill factor, open circuit voltage, and integral photocurrent for the corresponding solar cells. DSSC with 10 wt% of composite TiO_2 nanoparticles/TNTs film exhibited the highest light-to-electric energy conversion efficiency of 5.95%, short-circuit current density of 14.86 mA/cm^2 , open-circuit voltage of 0.68 V, and fill factor of 58.79%. These results indicate that the J_{SC} value increased significantly with the addition of the TNTs. However, the addition of TNTs had little influence on the open circuit voltage (V_{OC}) and the fill factor (FF). The observed increase in J_{SC} could be attributed to the increased electron lifetime in the one-dimensional electrode on the composite TiO_2 nanoparticles/TNTs film.

Table 1. The integral photocurrent density (J_{SC}), open circuit voltage (V_{OC}), fill factor (FF), and efficiency (η) of DSSCs fabricated using pure TiO_2 particles (bare) and using TiO_2 particles/TNTs with various compositions.

Sample	V_{OC} (V)	J_{SC} (mA/cm^2)	FF (%)	Efficiency ($\eta\%$)
Bare	0.67	12.93	58.43	5.11
TNT 5 wt%	0.67	13.37	58.56	5.30
TNT 10 wt%	0.68	14.86	58.79	5.95
TNT 15 wt%	0.68	14.31	58.71	5.71
TNT 20 wt%	0.67	12.52	58.25	4.92

Figure 4. Electrochemical impedance spectroscopy (EIS) Nyquist plots of DSSCs with TNT mixed TiO₂ films of different TNT concentrations. The following abbreviated terms were used: R_s (ohmic series resistance), R_{CT1} (3 charge-transfer resistance of the counter electrode), CPE1 (constant phase element of the counter electrode), R_{CT2} (4 charge-transfer resistance of the working electrode), CPE2 (constant phase element of the photoelectrode).

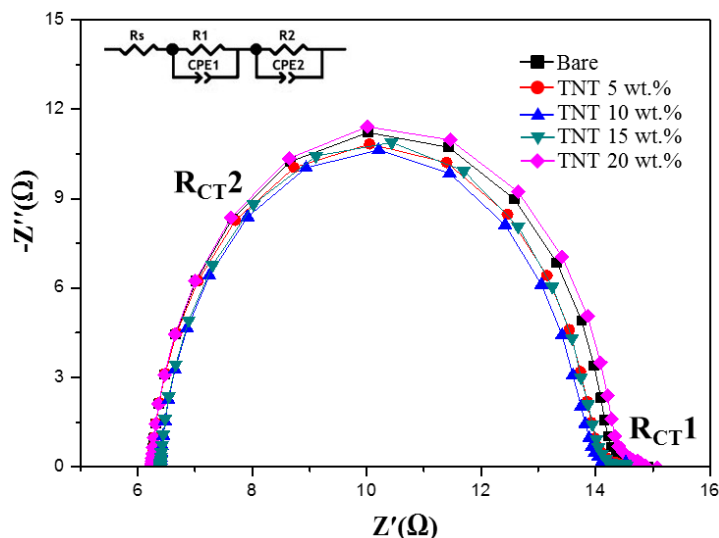
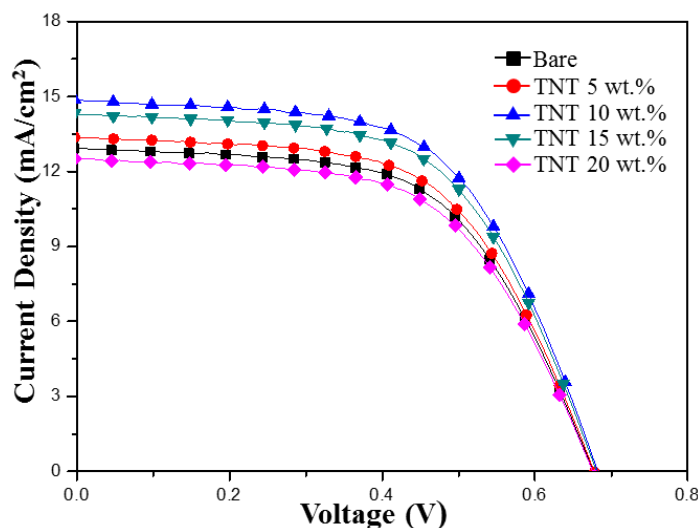
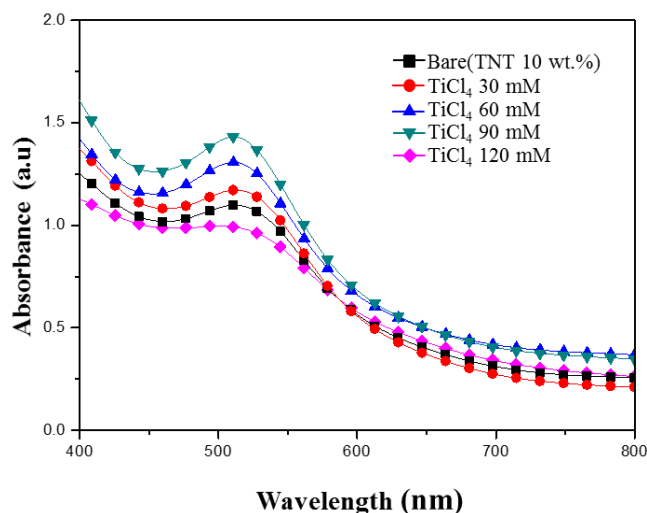


Figure 5. I - V characteristic of TiO₂ nanoparticle/TNT DSSCs.



DSSC with TNT (10 wt%) were referred as “Bare” condition (*i.e.*, internal reference) in the following measurements to investigate effect of TiCl₄ post treatment on DSSCs.

Figure 6 shows the absorption spectrum of N-719 dye in the 400–800 nm wavelength range in the various TiCl₄ post treatment (30–120 mM) TiO₂ films. At the wavelength 400–500 nm, the sample treated with a TiCl₄ concentration of 90 mM has the highest absorbance. It is reasonable that the TiCl₄ post treatment electrode provides more sites for dye absorption than the Bare (TNT 10 wt%), leading to a higher light harvesting and J_{sc} as expected.

Figure 6. UV-Vis absorbance of TiCl₄ post treated TiO₂ films for different TiCl₄ concentrations.

According to Lambert-Beer's law, higher absorbance means a higher dye concentration. A suitable amount of TiCl₄ in the film could provide a large surface area for dye adsorption. It is reported that small TiO₂ particles are formed on the surface of TiO₂ films by TiCl₄ post treatment and the surface area and the amount of dye adsorption are increased [19–23]. It is well known that the photocurrent of DSSCs is correlated directly with the number of dye molecules. Therefore, the increase of adsorbed dye molecules results in the increase of incident light being harvested and consequently a larger photocurrent.

In case of TiCl₄ post treatment with high concentration (120 mM), the absorbance was decrease. The post treatment with the high concentrations can lead the decrease of dye absorption of TiO₂ film due to the reduction of the film porosity by an increase of the nucleation in the nanoparticles. So, the inefficient charge-transfer paths increase the recombination rate of electrons, as a result, the photocurrent density and conversion efficiency can be decreased [24,25].

Figure 7 shows electrochemical impedance spectroscopy (EIS) Nyquist plots of DSSCs with a TiCl₄ post treatment. EIS is a useful method for the analysis of charge-transport processes and internal resistances [26]. As shown in Figure 7, there is a decrease in the charge-transfer resistance (R_{CT}) upon increasing the TiCl₄ ratio from 30 mM to 120 mM. This increases the number of injected electrons into the TiO₂ film, improves the electrical conductivity, and reduces the charge recombination at the TiO₂/dye/electrolyte interface [27,28]. R_{CT} becomes smaller when the TiCl₄ ratio increases. The reduction of R_{CT} means there is a decrease in the recombination rate and indicates fast electron-transfer processes in the DSSCs. The efficient charge-transfer paths decrease the recombination rate of electrons with I₃⁻ or the oxidizing dye, resulting in a high photocurrent density and conversion efficiency [24].

Figure 8 shows the $I-V$ characteristics of the TiO₂ film with the various TiCl₄-concentration post treatments. Two of the most important parameters for a solar cell are its photoelectric conversion efficiency and the fill factor (FF). When the $I-V$ curves approach a square shape, the FF is higher. In addition, solar cells with a high FF have a stable output voltage and current compared to the cell with the same V_{OC} and J_{SC} , and they produce more power. The photovoltaic properties of all post treated films are summarized in Table 2. J_{SC} increases with the amount of TiCl₄ until the TiCl₄ concentration

is 90 mM, beyond this limitation, J_{SC} decreases. J_{SC} increase was improved due to the increase of dye adsorption and it could be explained by the enhanced loading of dye molecules on TiO_2 films, which resulted in the improvement of J_{SC} , and a decrease in the charge-transfer resistance at interfaces. In the case of the $TiCl_4$ (120 mM), decrease of J_{SC} was result in low absorption of dye from the TiO_2 film to the photoelectrode.

The FF increased from 58% to 68% after $TiCl_4$ post treatment. With optimum post treatment conditions, the DSSCs fabricated on the $TiCl_4$ post treatment substrate showed an efficiency value of 7.83% due to an increased photocurrent density and fill factor.

Figure 7. EIS Nyquist plots of DSSCs with $TiCl_4$ post treated TiO_2 films for different $TiCl_4$ concentrations.

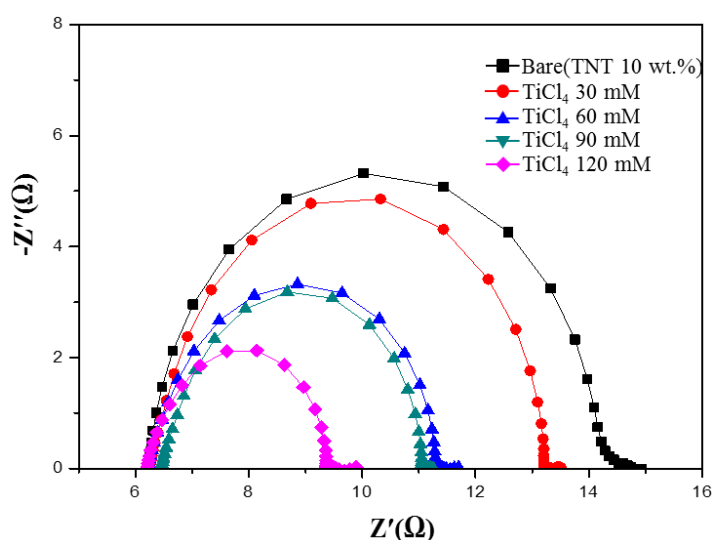


Figure 8. $I-V$ characteristic of $TiCl_4$ post treated DSSCs for different $TiCl_4$ concentrations.

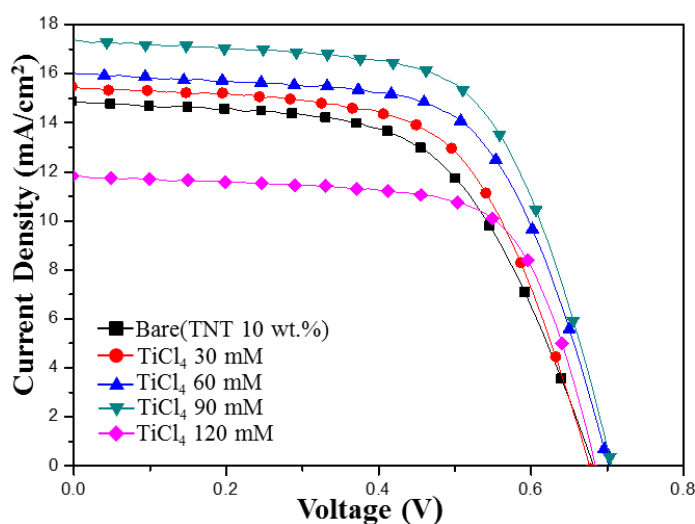


Table 2. The integral photocurrent density (J_{SC}), open circuit voltage (V_{OC}), fill factor (FF), and efficiency (η) of DSSCs fabricated using TiO_2 particles/TNTs 10 wt% (bare), and those fabricated using $TiCl_4$ post treatment.

Sample	V_{OC} (V)	J_{SC} (mA/cm ²)	FF (%)	Efficiency (η %)
Bare (TNT 10 wt%)	0.68	14.86	58.79	5.95
$TiCl_4$ 30 mM	0.67	15.45	61.37	6.42
$TiCl_4$ 60 mM	0.70	16.02	63.75	7.16
$TiCl_4$ 90 mM	0.70	17.37	63.84	7.83
$TiCl_4$ 120 mM	0.68	11.83	68.53	5.55

4. Conclusions

In this work, the improvement of performance on DSSCs using a $TiCl_4$ post-treatment on the TiO_2 films is proposed. The DSSCs were constructed with TiO_2 films made from TiO_2 nanoparticles and TNTs which were fabricated from an anodization process. Without post-treatment, DSSCs with light-to-electric energy conversion efficiency of 5.95% was achieved under a simulated solar light irradiation of 100 mW·cm² (AM 1.5). The DSSCs based on a TiO_2 nanoparticles/ TiO_2 nanotube composite showed a better photovoltaic performance (higher J_{SC}) than the cell purely made of TiO_2 nanoparticles. It was found that the conversion efficiency of DSSCs was highly affected by the properties of TNTs. The effect of a $TiCl_4$ post-treatment on the TiO_2 films was investigated using different the mole ratio of $TiCl_4$. DSSCs using TNTs and a $TiCl_4$ post treatment were measured to have a maximum conversion efficiency of 7.83% due to effective electron transport. Using TNTs (10 wt%) and a $TiCl_4$ (90 mM) post treatment process was found to be an effective method to improve the efficiency of TiO_2 nanoparticle based DSSCs.

Acknowledgments

This work was supported by the Human Resources Development program (No. 20124030200010) of the Korea Institute of Energy Technology Evaluation and Planning (KETEP) grant funded by the Korea government Ministry of Trade, Industry and Energy. This work was also supported by the National Research Foundation of Korea (NRF) Grant funded by the Korean Government (MEST) (No. 2012R1A1A2044472).

Author Contributions

The first author (Jun Hyuk Yang) carried out the laboratory test, the co-author (Kyung Hwan Kim; Chung Wung Bark) took charge of the small-scale laboratory measurement analysis, and the corresponding author (Hyung Wook Choi) have controlled the whole project.

Conflicts of Interest

The authors declare no conflict of interest.

References

1. O'Regan, B.; Grätzel, M. A low-cost, high-efficiency solar cell based on dye-sensitized colloidal TiO₂ films. *Nature* **1991**, *353*, 737–740.
2. Lee, B.; Kim, J. Enhanced efficiency of dye-sensitized solar cells by UV–O₃ treatment of TiO₂ layer. *Curr. Appl. Phys.* **2009**, *9*, 404–408.
3. O'Regan, B.; Grätzel, M. Optical electrochemistry I: Steady-state spectroscopy of conduction-band electrons in a metal oxide semiconductor electrode. *Chem. Phys. Lett.* **1991**, *183*, 89–93.
4. Durr, M.; Schmid, A.; Obermaier, M.; Rosselli, S.; Yasuda, A.; Nelles, G. Low-temperature fabrication of dye-sensitized solar cells by transfer of composite porous layers. *Nature* **2005**, *4*, 607–611.
5. Matsui, H.; Okada, K.; Kawashima, T.; Ezure, T.; Tanabe, N.; Kawano, R.; Watanabe, M. Application of an ionic liquid-based electrolyte to a 100 mm × 100 mm sized dye-sensitized solar cell. *J. Photochem. Photobiol. A Chem.* **2004**, *164*, 129–135.
6. Kim, S.S.; Nah, Y.C.; Noh, Y.Y.; Jo, J.; Kim, D.Y. Electrodeposited Pt for cost-efficient and flexible dye-sensitized solar cells. *Electrochim. Acta* **2006**, *51*, 3814–3819.
7. Robertson, N. Optimizing Dyes for Dye-Sensitized Solar Cells. *Int. Ed.* **2006**, *45*, 2339–2345.
8. Xu, C.; Shin, P.H.; Cao, L.; Wu, J.; Gao, D. Ordered TiO₂ Nanotube Arrays on Transparent Conductive Oxide for Dye-Sensitized Solar Cells. *Chem. Mater.* **2010**, *22*, 143–148.
9. Stergiopoulos, T.; Valota, A.; Likodimos, V.; Speliotis, T.; Niarchos, D.; Skeldon, P.; Thompson, G.E.; Falaras, P. Dye-sensitization of self-assembled titania nanotubes prepared by galvanostatic anodization of Ti sputtered on conductive glass. *Nanotechnology* **2009**, *20*, doi:10.1088/0957-4484/20/36/365601.
10. Crossland, E.J.W.; Nedelcu, M.; Ducati, C.; Ludwigs, S.; Hillmyer, M.A.; Steiner, U.; Snaith, H.J. Block Copolymer Morphologies in Dye-Sensitized Solar Cells: Probing the Photovoltaic Structure–Function Relation. *Nano Lett.* **2009**, *9*, 2813–2819.
11. Kang, T.S.; Smith, A.P.; Taylor, B.E.; Durstock, M.F. Fabrication of Highly-Ordered TiO₂ Nanotube Arrays and Their Use in Dye-Sensitized Solar Cells. *Nano Lett.* **2009**, *9*, 601–606.
12. Foong, T.R.B.; Shen, Y.; Hu, X.; Sellinger, A. Template-Directed Liquid ALD Growth of TiO₂ Nanotube Arrays: Properties and Potential in Photovoltaic Devices. *Funct. Mater.* **2010**, *20*, 1390–1396.
13. Yoon, J.H.; Jang, S.R.; Vittal, R.; Lee, J.; Kim, K.J. TiO₂ nanorods as additive to TiO₂ film for improvement in the performance of dye-sensitized solar cells. *J. Photochem. Photobiol. A Chem.* **2006**, *180*, 184–188.
14. Kang, S.H.; Choi, S.H.; Kang, M.S.; Kim, J.Y.; Kim, H.S.; Hyeon, T.; Sung, Y.E. Nanorod-Based Dye-Sensitized Solar Cells with Improved Charge Collection Efficiency. *Adv. Mater.* **2008**, *20*, 54–58.
15. Pan, K.; Dong, Y.; Tian, C.; Zhou, W.; Tian, G.; Zhao, B.; Fu, H. TiO₂-B narrow nanobelt/TiO₂ nanoparticle composite photoelectrode for dye-sensitized solar cells. *Electrochim. Acta* **2009**, *54*, 7350–7356.

16. Mikroyannidis, J.A.; Strlianakis, M.M.; Roy, M.S.; Suresh, P.; Sharma, G.D. Synthesis, photophysics of two new perylene bisimides and their photovoltaic performances in quasi solid state dye sensitized solar cells. *J. Power Sources* **2009**, *194*, 1171–1179.
17. Bay, L.; West, K.; Jensen, B.W.; Jacobsen, T. Electrochemical reaction rates in a dye-sensitized solar cell—the iodide/tri-iodide redox system. *Sol. Energy Mater. Sol. Cells* **2006**, *90*, 341–351.
18. Lin, L.Y.; Lee, C.P.; Vittal, R.; Ho, K.C. Selective conditions for the fabrication of a flexible dye-sensitized solar cell with Ti/TiO₂ photoanode. *J. Power Sources* **2010**, *195*, 4344–4349.
19. Lee, S.H.; Chae, S.Y.; Hwang, Y.J.; Koo, K.-K.; Joo, O.-S. Influence of TiO₂ nanotube morphology and TiCl₄ treatment on the charge transfer in dye-sensitized solar cells. *Appl. Phys. A Mater. Sci. Process.* **2013**, *112*, 733–737.
20. Meen, T.-H.; Jhuo, Y.-T.; Chao, S.-M.; Lin, N.-Y.; Ji, L.-W.; Tsai, J.-K.; Wu, T.-C.; Chen, W.-R.; Water, W.; Huang, C.-J. Effect of TiO₂ nanotubes with TiCl₄ treatment on the photoelectrode of dye-sensitized solar cells. *Nanoscale Res. Lett.* **2012**, *7*, 1–5.
21. Sommeling, P.M.; O'Regan, B.C.; Haswell, R.R.; Smit, H.J.P.; Bakker, N.J.; Smits, J.J.T.; Kroon, J.M.; van Roosmalen, J.A.M. Influence of a TiCl₄ post-treatment on nanocrystalline TiO₂ films in dye-sensitized solar cells. *J. Phys. Chem. B* **2006**, *110*, 19191–19197.
22. Park, N.-G.; Schlichthorl, G.; van de Lagemaat, J.; Cheong, H.M.; Mascarenhas, A.; Frank, A.J. Dye-sensitized TiO₂ solar cells: Structural and photoelectrochemical characterization of nanocrystalline electrodes formed from the hydrolysis of TiCl₄. *J. Phys. Chem. B* **1999**, *103*, 3308–3314.
23. Barbe, C.J.; Arendse, F.; Comte, P.; Jirousek, M.; Lenzenmann, F.; Shklover, V.; Grätzel, M. Nanocrystalline titanium oxide electrodes for photovoltaic applications. *J. Am. Ceram. Soc.* **1997**, *80*, 3157–3171.
24. Zhong, M.; Shi, J.; Zhang, W.; Han, H.; Li, C. Charge recombination reduction in dye-sensitized solar cells by depositing ultrapure TiO₂ nanoparticles on “inert” BaTiO₃ films. *Mater. Sci. Eng. B* **2011**, *176*, 1115–1122.
25. Xu, W.; Dai, S.; Hu, L.; Zhang, C.; Xiao, S.; Luo, X.; Jing, W.; Wang, K. Influence of Different Surface Modifications on the Photovoltaic Performance and Dark Current of Dye-Sensitized Solar Cells. *Plasma Sci. Technol.* **2007**, *9*, doi:10.1088/1009-0630/9/5/08.
26. Yang, C.C.; Zhang, H.Q.; Zheng, Y.R. DSSC with a novel Pt counter electrodes using pulsed electroplating techniques. *Curr. Appl. Phys.* **2011**, *11*, S147–S153.
27. Fabregat-Santiago, F.; Bisquert, J.; Palomares, E.; Otero, L.; Kuang, D.; Zakeeruddin, S.M.; Grätzel, M. Correlation between Photovoltaic Performance and Impedance Spectroscopy of Dye-Sensitized Solar Cells Based on Ionic Liquids. *J. Phys. Chem. C* **2007**, *111*, 6550–6560.
28. Kern, R.; Sastrawan, R.; Ferber, J.; Stangl, R. Modeling and interpretation of electrical impedance spectra of dye solar cells operated under open-circuit conditions. *J. Luther Electrochim. Acta* **2002**, *47*, 4213–4225.